Thermal Hall effect from a modified Lorentz gas model

Hongyuan Chen, Yu Yang, Zhizhou Yu, Ming Zhong,* and Lifa Zhang†
NNU-SULI Thermal Energy Research Center (NSTER) and Center for Quantum Transport and Thermal Energy Science (CQTES), School of Physics and Technology, Nanjing Normal University, Nanjing 210023, China

(Received 9 September 2019; revised manuscript received 12 March 2020; accepted 2 April 2020; published 23 April 2020)

We systematically investigate the thermal Hall effect in a Lorentz gas model with rotating circular scatterers; the rotating scatterers play a role similar to the magnetic field. The modified Lorentz gas model is a normal thermal transport system that satisfies Fourier law: the thermal conductivity is independent of the model length. We find that the intensity of the Hall effect changes its sign when the rotating direction of disks changes and it is independent of the magnitude of longitudinal temperature difference and only dependent of the average longitudinal temperature: it decreases with increasing the average temperature, especially at low angular velocity. The thermal Hall effect found in the modified Lorentz gas will help us understand the mechanism of the thermal Hall system and provide guidance for the application of the thermal Hall effect.

DOI: 10.1103/PhysRevE.101.042129

I. INTRODUCTION

Thermal transport has received much attention in recent years due to its potential applications in thermal devices such as thermal diodes [1–3] and thermal transistors [4]. As an important carrier of heat transport, phonons have been extensively studied and found many important properties, such as the thermal Hall effect [5–19]. The classical Hall effect is the production of a voltage difference across an electrical conductor, transverse to an electric current in the conductor and an applied magnetic field perpendicular to the current. The thermal Hall effect, as an analog of the classical Hall effect, also generates a transverse heat flow by a longitudinal temperature gradient, causing the heat flow to distort.

A phonon-mediated thermal Hall effect has been demonstrated experimentally in the paramagnetic dielectric by applying a magnetic field perpendicular to the heat flow [5,6]. These results are very surprising because phonons are electrically neutral quasiparticles that do not change the direction of transmission under the Lorentz force of the magnetic field. Subsequent theories point out that phonons are also carriers with angular momentum [20]. Through Raman spin-phonon interaction, the magnetic field can produce an effective force for distorting phonon transmission [7–10]. The physical image of the thermal Hall effect can also be understood by the acoustic Faraday effect: the magnetic field splits the phonon dispersion into paramagnetic and diamagnetic branches which causes a rotation of the Rayleigh pattern in the phonon scattering cross section [5].

It is well known that the Lorentz gas model can simulate the heat transport. The Lorentz gas model was first employed by Alonso in 1999 to study the heat conduction of a dynamical system [21]. It is based on the classical collision of rigid body balls with two parallel borderlines to simulate transport properties of noninteracting elastic particles. The particle in Lorentz channel has ergodic properties, so it can display characteristic phenomenon of classical transport. This model has been developed to reflect the transport properties of many systems [22–28]. Now, it can be employed to study many classical thermal transport problems, such as heat conduction of layered structures [29,30] and boundary effects on thermal conductivity [31]. Then we will ask naturally, in a Lorentz gas model, if adding a scattering medium, like rotating disks, can these scatters work like the magnetic field in the thermal Hall effect system? And will this Lorentz gas system be able to simulate the thermal Hall effect?

In this paper, we construct a simple and clear model to simulate the thermal Hall effect system, in which particles are considered as phonon and rotating disks are considered as a magnetic field. The disks twist the direction of particles in our model. That is the physical essence of thermal Hall effect, in which the magnetic field changes the direction of phonon by coupling spin and orbit. We first study the thermal transport in a classical system based on the Lorentz gas model and the length independent thermal conductivity is found. The thermal Hall effect is then investigated by introducing the rotating disk scatters into the classical model. And we successfully simulate the thermal Hall effect. We find that the relative Hall temperature difference changes its sign when the disk scatters change their rotating direction. Moreover, we use this model to study the characteristics and regulation of the thermal Hall effect. And the results are compared with previous works.

II. SIMULATION METHOD

The schematic setup of the classical Lorentz gas model is plotted in Fig. 1(a). First, a particle (phonon) is emitted

*mzhong@njnu.edu.cn
†phyzlf@njnu.edu.cn

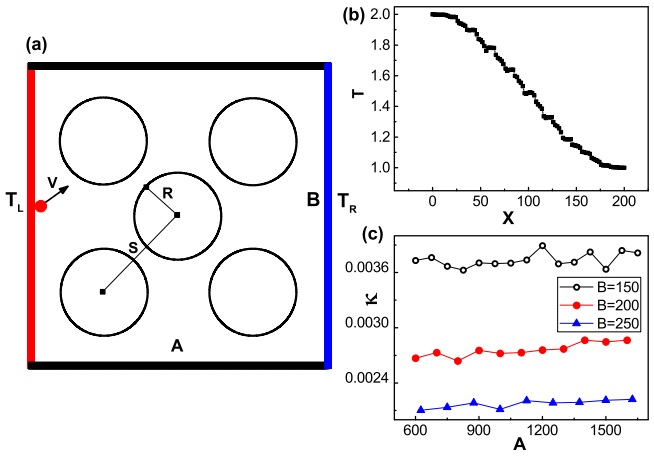

FIG. 1. (a) Schematic setup of the classical model. A rectangle with a length of A and a width of B. The upper and lower ends are elastic collision boundaries. The hard disk scatters are placed between two reservoirs. The radius of disks is R and the distance between the centers of two adjacent disks is S. (b) Linear temperature gradients are obtained. The temperature distribution along the transmission direction in the classical model with $A = B = 200$ in which 181 hard disks are placed. The left and right ends are isothermal heat reservoirs with temperatures $T_L = 2$ and $T_R = 1$, respectively. (c) The thermal conductivity κ as the function of model length A in the classical model. The model width is chosen to be $B = 150$ (black open circles), $B = 200$ (red solid circles), and $B = 250$ (blue triangles). The thermal conductivity is almost independent of the model length.

from the left heat reservoir with temperature $T = T_L$ with the following velocity distributions [1,2]:

$$P(v_\parallel) = \frac{|v_\parallel|}{T} e^{-v_\parallel^2/(2T)}, \tag{1}$$

$$P(v_\perp) = \frac{1}{\sqrt{2\pi T}} e^{-v_\perp^2/(2T)}, \tag{2}$$

where $v_\parallel$ and $v_\perp$ are the x- and y-axis components of the velocity. For simplicity, dimensionless units are used here. Both the Boltzmann constant (k_B) and the particle mass (m) are set as 1. The positions where a particle emanates are random in the heat reservoir.

The hard disk scatters fixed on a triangular lattice are placed between two heat reservoirs. The radius of disks is chosen as $R = \sqrt{3}S/4$ known in the literature as the critical horizon [30], where S is the distance between the centers of disks. Specifically, the center points of five hard disks are fixed at $(A/4, 3B/4)$, $(A/4, B/4)$, $(A/2, B/2)$, $(3A/4, 3B/4)$, and $(3A/4, B/4)$) with the length A and the width B of our model. The particle undergoes perfect elastic collision among the nonspinning hard disk scatters, lower and upper boundaries, before arriving at the thermal reservoirs where it will be absorbed. Then a new particle satisfying the velocity distributions of Eqs. (1) and (2) with temperature $T = T_R$ should be released from the right reservoir. This process will circulate for enough time so heat can be transmitted steadily from the left reservoir with a higher temperature to the right one with a lower temperature.

In order to compute the temperature distribution, the whole space of our Lorentz gas model is divided into equidistant partitions along the transport direction. Then the temperature distribution T_m in the transmission direction, the steady heat flow I, and the thermal conductivity κ can be calculated as [31]

$$T_m = \frac{2}{3} E_m, \tag{3}$$

$$I = \frac{\Sigma_n \Delta E^n}{t}, \tag{4}$$

$$\kappa = \frac{AI}{B\Delta T}. \tag{5}$$

Here, T_m and E_m represent the temperature and average kinetic energy of the mth region, respectively. The space of our model is divided into 100 regions and the kinetic energy of the particle is taken as the total energy of the particle since the interaction between particles is not considered. In Eqs. (4) and (5), t is the total time and ΔT is the temperature difference between two heat reservoirs. In our model, the energy of a particle changes only when the particle is absorbed by a reservoir. So $\Delta E^n = E^n_{in} - E^n_{out}$ is the change of energy of nth time the particle was absorbed and rereleased by a reservoir. In our simulation, the system is considered to be thermal nonequilibrium stationary state when the mean value of heat flow in 1000 transports has a difference within 10^{-8} with heat flow in all formal transports; we can take the system as in thermal nonequilibrium stationary state.

Figure 1(b) presents the temperature distribution along the transport direction in which the linear gradient in temperature distribution is obtained. The thermal conductivity is also computed and it is found that the thermal conductivity is independent of the system length and only decreases with the increasing model width, as shown in Fig. 1(c), which implies that the thermal conductivity is an intrinsic parameter of the model. These results confirm that our model satisfies the normal thermal transport case.

In order to study the thermal Hall effect, the rotating disks model is then introduced, as shown in Fig. 2(a). In contrast to the classical model, the disk scatters are rotating with the same and constant angular velocity ω and the upper and lower boundaries are replaced by two heat reservoirs with the temperature $T_3 = (T_L + T_R)/2$. When a particle collides with the upper and lower boundaries, it goes through the same process as that with the left and right boundaries. That means the distribution of $v_\perp$ and $v_\parallel$ follows Eq. (1) and Eq. (2), respectively. The collisions between a particle and disks are still perfect elastic. By considering the moment of inertia of disks as infinite and the energy of particles as a constant, the collision process can be described as

$$v_{n,i} = -\alpha_i v_{n,i-1}, \quad v_{t,i} = \alpha_i(\beta R\omega + v_{t,i-1}), \tag{6}$$

where $v_{n,i}$ and $v_{t,i}$ is the normal velocity and tangential velocity relative to the disk after the ith collision, respectively. ω is the rotating angular velocity of disks. The coefficients α and β are used to describe the viscosity of the disk. α can be

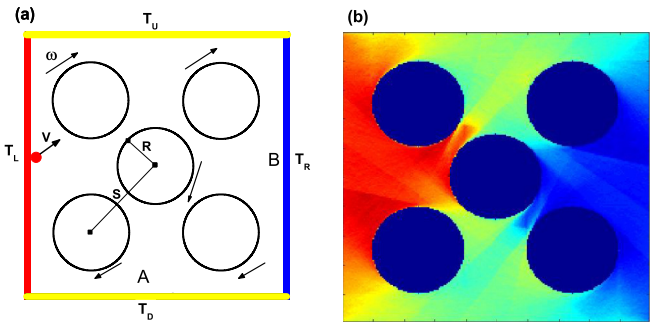

FIG. 2. (a) Schematic setup of the modified model. On the basis of the classical model, the upper and lower ends are replaced by isothermal heat reservoirs with a temperature of $T_U = T_D = T_3$. The disk scatters are rotating with a fixed angular velocity ω. (b) The two-dimensional temperature distribution of the modified model. The temperature vortices have the same rotating direction as that of disks. The temperature of the red region is higher than that of the blue region.

obtained as

$$\alpha_i = \sqrt{\frac{v_{n,i-1}^2 + v_{t,i-1}^2}{v_{n,i-1}^2 + (\beta R\omega + v_{t,i-1})^2}}. \tag{7}$$

Here we take β as constant 1; a smaller β means ω is smaller. And if $\omega = 0$, then $\alpha = 1$, and the model will be a perfect elastic collision model. Equation (6) and Eq. (7) can be understood that both the normal velocity and tangential velocity are normalized by α and β when a collision happens to keep the conservation of total kinetic energy of particles. The kinetic energy and the rotating speed should be kept constant. On the one hand, if the rotating speed of disks is fixed and the kinetic energy of the particle can change, then disks are equivalent to the reservoirs with a higher temperature than four boundaries. In this way, all the boundary reservoirs will absorb heat. There will be no Hall effect. On the other hand, if the kinetic energy is not conserved, the rotating speed of disks will change; then the initial rotation of disks will have no effect on the whole system in long time. Also no Hall effect exists. It is the only way to keep the kinetic energy of the particles and the rotating speed of disks constant, so that the effect of disks is similar to that of the magnetic field. The only changes we can do are to use different velocity change formulas during collisions with disks [Eqs. (6) and (7)] to describe different actions of magnetic fields.

Figure 2(b) presents the two-dimensional temperature profile of our model with rotating disks. The temperature vortices are consistent with the rotation direction of disks. Then we compute the time-dependent heat flows of four reservoirs (see Fig. 3). Apart from the longitudinal heat flow, a transverse flow between the upper and lower reservoirs is obtained. And the transverse flow is much smaller than the longitudinal one. When the disk rotates clockwise, the heat flows of upper and right reservoirs are positive, which means these two reservoirs absorb heat energies. Obviously, the total heat flow of four reservoirs is zero.

In order to further study the transverse flow in the case with clockwise rotating disks, the relation between the transverse

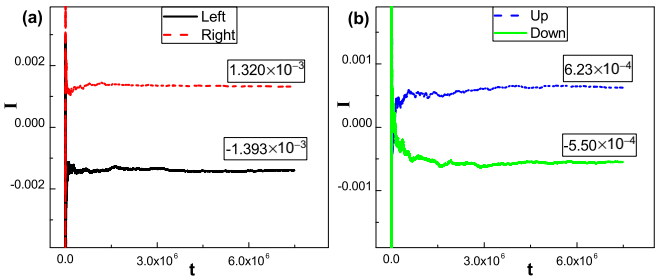

FIG. 3. Time-dependent heat flow of (a) left and right reservoirs in the longitudinal direction and (b) upper and lower reservoirs in the transverse direction. The positive heat flow indicates the energy absorption of the corresponding reservoirs.

heat flow I_{DU} and the rotating angular velocity ω is plotted in Fig. 4(a). Where $I_{\mathrm{DU}} = I_U - I_D$, I_U donates the energy change of the up reservoir and I_D donates the energy change of the down one. It is found that I_{DU} is negative for $\omega < 0$, while I_{DU} is positive for $\omega > 0$ and I_{DU} increases with the increasing rotating angular velocity. This behavior is qualitatively similar to the inverse tangent function. To quantitatively describe the thermal Hall effect, external transverse temperature gradients are applied to make the transverse heat flow vanish ($I_{\mathrm{DU}} = I_U = I_D = 0$). The relation between the transverse temperature difference ΔT_{UD} and the rotating angular velocity is plotted in Fig. 4(b). Here, the average external transverse temperature is 1.5. The transverse temperature difference changes its sign at $\omega = 0$, which shows the same behavior as the transverse heat flow. Our computing results well agree

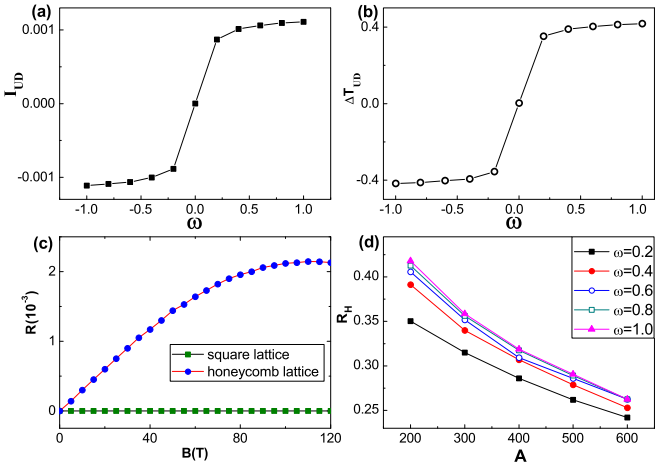

FIG. 4. (a) Transverse heat flow I_{DU} as the function of the rotating angular velocity ω. (b) The external transverse temperature difference ΔT_{UD} as the function of the rotating angular velocity ω that makes the transverse heat flow vanish. (c) The relative Hall temperature difference as the function of the magnetic field. This graph is from Ref. [9]. (d) The relative Hall temperature difference R_H as the function of the model length A. The rotating angular velocity of disks are chosen to be $\omega = 0.2$ (black solid squares), $\omega = 0.4$ (red solid circles), $\omega = 0.6$ (blue open circles), $\omega = 0.8$ (cyan open squares), and $\omega = 1.0$ (magenta triangles). The relative Hall temperature difference R_H decreases with the increasing model length A.

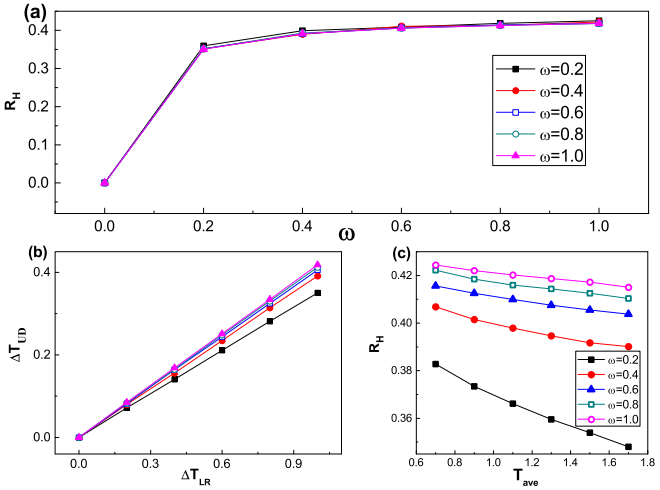

FIG. 5. (a) Relative Hall temperature difference R_H as the function of the rotating angular velocity ω with different longitudinal temperature difference $\Delta T_{\rm LR}$ and a fixed average longitudinal temperature $T_{\rm ave} = 1.5$. The relative Hall temperature difference is independent of the longitudinal temperature difference. (b) The relation between the transverse temperature difference $\Delta T_{\rm UD}$ and the longitudinal temperature difference $\Delta T_{\rm LR}$. The transverse temperature difference $\Delta T_{\rm UD}$ shows linear dependence with the longitudinal temperature difference $\Delta T_{\rm LR}$. The slope of each curve indicates the relative Hall temperature difference. (c) The relative Hall temperature difference R_H as the function of the average longitudinal temperature $T_{\rm ave}$ with a fixed transverse temperature difference $\Delta T_{\rm UD} = 1$.

with theoretical calculations of phonon Hall effect in a honeycomb lattice using an exact nonequilibrium Green's function formulation [9] [see Fig. 4(c)] and the first phonon Hall effect experiment [5].

To describe the intensity of thermal Hall effect, we define the relative Hall temperature difference R_H as

$$R_H = \frac{\Delta T_{\rm UD}}{\Delta T_{\rm LR}}. \tag{8}$$

Here, $\Delta T_{\rm LR}$ and $\Delta T_{\rm UD}$ are the applied external longitudinal and transverse temperature differences, respectively. In Fig. 4(d), we present the length dependent relative Hall temperature difference. The relative Hall temperature difference decreases with the increasing model length and the decreasing rate is almost independent of the rotating angular velocity. It also indicates that when the length A is long enough, the relative Hall temperature difference has a weak relationship with rotating speed. This is because, when A is very long, although the effect of every single rotation is very weak, the relative Hall temperature difference becomes saturated as the particles go through lots of rotations.

Finally, the influence of longitudinal temperature on the thermal Hall effect is studied. Figure 5(a) presents the relative Hall temperature difference as the function of the rotating angular velocity with different $\Delta T_{\rm LR}$ and a fixed average longitudinal temperature $T_{\rm ave} = \frac{T_L+T_R}{2}$ of left and right reservoirs. We find that R_H is independent of the longitudinal temperature difference $\Delta T_{\rm LR}$ at a certain rotating angular velocity, as shown in Fig. 5(b). That indicates the transverse temperature difference has a linear response to the longitudinal one. This is the intrinsic property of the thermal Hall effect. R_H as the function of the average longitudinal temperature $T_{\rm ave}$ with a fixed $\Delta T_{\rm LR}$ is plotted in Fig. 5(c). For the system with a small rotating angular velocity, R_H decreases with the increasing $T_{\rm ave}$. This is because, when $T_{\rm ave}$ is larger, the particle velocity becomes larger. Then the transport direction of particles is hard to change by the rotating disks, which leads to a small transverse flow and a corresponding small R_H. It also indicates that if the longitudinal average temperature is large enough under a given rotating speed, the longitudinal transport will take control. Our results are consistent with the experimental observation of magnon Hall effect [32–34], in which the thermal Hall conductivity declines when temperature rises from 50 K to the Curie point. However, when the rotating angular velocity increases, the decreasing rate of R_H reduces rapidly. R_H becomes saturated with the increasing ω and almost does not change by the average longitudinal temperature at a large rotating angular velocity since the ability of rotating disks to change the transport direction of particles becomes saturated when the rotating angular velocity becomes large.

III. DISCUSSION ABOUT SOME EXPERIMENTAL RESULTS

The value of transverse temperature difference in Fig. 4(b) is equal to 1, so the y axis is the relative Hall temperature difference, the same y axis as Fig. 4(c). As we can see, the results of the modified Lorentz gas model [Fig. 4(b)] are qualitatively similar to the theoretical results of phonon Hall effect in a honeycomb lattice [Fig. 4(c)]. Moreover, both theoretical [9] and experimental [5] results show that the relative Hall temperature difference is proportional to the magnetic field. In our model, if the rotating speed is small, the particles will be trapped between the disks for a long time, or even have a periodic trajectory, as mentioned in [35]. Then it is almost impossible to calculate particle transport since the particles are very difficult to get out. However, from the curve trend in Fig. 4(b) we can see that the relative Hall temperature difference can behave nearly linear with the rotating speed.

The thermal Hall effect in our modified Lorentz gas model has many similar properties with phonon Hall effect and magnon Hall effect. This is a simple and clear model to understand thermal Hall effect.

IV. CONCLUSION

In summary, we study the thermal transport in a classical Lorentz gas model with the hard nonspinning disk scatterers. The modified Lorentz gas model is a normal thermal transport system that satisfies Fourier law: the thermal conductivity is independent of the model length. The thermal Hall effect is then investigated by introducing the rotating disks as nonlinear scatterers. The two-dimensional temperature profile is computed and the temperature vortex shows the same rotating direction with that of the disk scatters. We find the relative Hall temperature difference changes its sign when the rotating direction of disks changes and it decreases with the increasing model length. Moreover, the influence of longitudinal tem-

perature on the relative Hall temperature difference is investigated. We find that the transverse temperature difference has a linear response to the longitudinal temperature difference. And the intensity of the Hall effect decreases with the average longitudinal temperature.

ACKNOWLEDGMENTS

This work was financially supported by the National Natural Science Foundation of China (Grants No. 11890703, No. 11574154, and No. 11704190) and the Jiangsu Provincial Natural Science Foundation of China (Grant No. BK20171030).

[1] B. Li, L. Wang, and G. Casati, Phys. Rev. Lett. **93**, 184301 (2004).
[2] C. W. Chang, D. Okawa, A. Majumdar, and A. Zettl, Science **314**, 1121 (2006).
[3] Y. Yang, H. Chen, H. Wang, N. Li, and L. Zhang, Phys. Rev. E **98**, 042131 (2018).
[4] B. Li, L. Wang, and G. Casati, Appl. Phys. Lett. **88**, 143501 (2006).
[5] C. Strohm, G. L. J. A. Rikken, and P. Wyder, Phys. Rev. Lett. **95**, 155901 (2005).
[6] A. V. Inyushkin and A. N. Taldenkov, JETP Lett. **86**, 379 (2007).
[7] M. Mori, A. Spencer-Smith, O. P. Sushkov, and S. Maekawa, Phys. Rev. Lett. **113**, 265901 (2014).
[8] Y. Kagan and L. A. Maksimov, Phys. Rev. Lett. **100**, 145902 (2008).
[9] L. Zhang, J. Wang, and B. Li, New J. Phys. **11**, 113038 (2009).
[10] L. Zhang and Q. Niu, Phys. Rev. Lett. **112**, 085503 (2014).
[11] T. Qin, Q. Niu, and J. Shi, Phys. Rev. Lett. **107**, 236601 (2011).
[12] L. Sheng, D. N. Sheng, and C. S. Ting, Phys. Rev. Lett. **96**, 155901 (2006).
[13] L. Zhang, J. Ren, J. S. Wang, and B. Li, Phys. Rev. Lett. **105**, 225901 (2010).
[14] T. Qin, J. Zhou, and J. Shi, Phys. Rev. B **86**, 104305 (2012).
[15] L. Zhang, J. Ren, J. Wang, and B. Li, J. Phys.: Condens. Matter **23**, 305402 (2011).
[16] J. S. Wang and L. Zhang, Phys. Rev. B **80**, 012301 (2009).
[17] B. Agarwalla, L. Zhang, J. Wang, and B. Li, Eur. Phys. J. B **81**, 197 (2011).
[18] L. Zhang, New J. Phys. **18**, 103039 (2016).
[19] L. Zhang, J. Ren, J. S. Wang, and B. Li, Phys. Rev. B **87**, 144101 (2013).
[20] L. Zhang and Q. Niu, Phys. Rev. Lett. **115**, 115502 (2015).
[21] D. Alonso, R. Artuso, G. Casati, and I. Guarneri, Phys. Rev. Lett. **82**, 1859 (1999).
[22] B. Moran, W. G. Hoover, and S. Bestiale, J. Stat. Phys. **48**, 709 (1987).
[23] B. Li, G. Casati, and J. Wang, Phys. Rev. E **67**, 021204 (2003).
[24] Y. G. Sinai, Funct. Anal. Its. Appl. **13**, 192 (1979).
[25] H. Wang, Y. Yang, H. Chen, N. Li, and L. Zhang, Phys. Rev. E **99**, 062111 (2019).
[26] D. F. M. Oliveira, J. Vollmer, and E. D. Leonel, Physica D **240**, 389 (2011).
[27] L. A. Bunimovich and Y. G. Sinai, Commun. Math. Phys. **78**, 247 (1980).
[28] L. A. Bunimovich and Y. G. Sinai, Commun. Math. Phys. **78**, 479 (1981).
[29] G. Casati, C. Mejia-Monasterio, and T. Prosen, Phys. Rev. Lett. **98**, 104302 (2007).
[30] H. Larralde, F. Leyvraz, and C. M. Monasterio, J. Stat. Phys. **113**, 197 (2003).
[31] H. Chen, H. Wang, Y. Yang, N. Li, and L. Zhang, Phys. Rev. E **98**, 032131 (2018).
[32] Y. Onose, T. Ideue, H. Katsura, Y. Shiomi, N. Nagaosa, and Y. Tokura, Science **329**, 297 (2010).
[33] T. Ideue, Y. Onose, H. Katsura, Y. Shiomi, S. Ishiwata, N. Nagaosa, and Y. Tokura, Phys. Rev. B **85**, 134411 (2012).
[34] A. Mook, J. Henk, and I. Mertig, Phys. Rev. B **89**, 134409 (2014).
[35] J. Machta and R. Zwanzig, Phys. Rev. Lett. **50**, 1959 (1983).